EUROfusion

WPMAT-PR(18) 19291

H. Gietl et al.

Textile preforms for tungsten fibre-reinforced composites

Preprint of Paper to be submitted for publication in
Journal of Composite Materials

This work has been carried out within the framework of the EUROfusion Consortium and has received funding from the Euratom research and training programme 2014-2018 under grant agreement No 633053. The views and opinions expressed herein do not necessarily reflect those of the European Commission.

Textile preforms for tungsten fibre-reinforced composites

Journal Title
XX(X):1–9

DOI: 10.1177/ToBeAssigned
www.sagepub.com/
SAGE

H. Gietl[1,2], A. v. Müller [1,2], J.W. Coenen [3], M. Decius [4,*], D. Ewert [5],T. Höschen [1], Ph. Huber [4], M. Milwich [5], J. Riesch [1] and R. Neu [1,2]

Abstract

Demanding high heat flux applications, as for example plasma-facing components of future nuclear fusion devices, ask for the development of advanced materials. For such components, copper alloys are currently regarded as heat sink materials while monolithic tungsten is foreseen as directly plasma-facing material. However, the combination of these materials in one component is problematic since they exhibit different thermomechanical characteristics and their optimum operating temperatures do not overlap. In this context, an improvement can be achieved by applying composite materials that make use of drawn tungsten fibres as reinforcement. For the manufacturing processes of these composites, suitable tungsten fibre preform production methods are needed. In the following, we will show that tungsten fibres can be processed to suitable preforms by means of well-established textile techniques as studies regarding the production of planar weavings (wire distances of 90-271μm), circular braidings (multi-layered braidings with braiding angle of 60° and 12°) as well as multifilamentary yarns (15 tungsten filaments with 16 μm diameter) are presented. With such different textile preforms tungsten fibre-reinforced tungsten (W_f/W) with a density of over 99% and pore free tungsten fibre-reinforced copper W_f/Cu were produced which proves their applicability with respect to a composite material production processes.

Keywords

Tungsten fibre, Tungsten fibre fabric, Tungsten fibre braiding, Tungsten fibre yarn, Metal-matrix composites (MMCs)

Introduction

When considering the increase of energy consumption with the future growth of human population new advanced methods to produce energy with a reduced amount of environmental impact are necessary. One possibility in this respect could be the use of controlled nuclear fusion reactions (1; 2). The next step towards a future fusion power plant will be the experimental reactor ITER which is designed to produce ten times more thermal power than is injected into the plasma and which is currently under construction. The foreseen successor of ITER is a fusion demonstration power plant (DEMO) which is presently being conceptually designed (3). In such advanced fusion reactors, deuterium and tritium are fused to an alpha particle and a fast neutron within a magnetically confined plasma (4). In a fusion reactor, the materials surrounding the fusion plasma need to exhibit diverse properties in order to withstand the loading conditions due to the interaction with the plasma (5; 6). The components which will be facing a fusion plasma are supposed to sustain severe cyclic particle and heat loads up to 20 MW/m^2 (7; 8). Furthermore, neutron irradiation leading to degradation of thermophysical and mechanical material properties is a crucial aspect (9; 10). For the plasma-facing component (PFC) in the highly loaded parts of ITER a design as proposed in (11) is foreseen. Within that design, tungsten (W) is foreseen as plasma-facing material (PFM) while the copper (Cu) alloy CuCrZr is the designated heat sink material and water is selected as coolant (5). Tungsten is one of the most promising PFM for fusion applications mainly due to the high threshold energy for erosion and the low retention of tritium in the material (5; 7). However, the main drawbacks of monolithic W are a high ductile-to-brittle transition temperature (DBTT) of up to 800 °C (12) as well as embrittlement by recrystallization and extensive grain growth above 1250 °C (13). These are the boundaries that define the optimal operating temperature range of W which is illustrated in Fig. 1. As W has this temperature limitations, different advanced material concepts for such applications are currently under development (14). Within a PFC (Fig. 2), as mentioned before, W has to be joined to a heat sink where Cu alloys are currently regarded as appropriate. Especially, the precipitation hardened Cu alloy CuCrZr is foreseen for this application (11; 15; 16; 17). The commended operating

[1]Max-Planck-Institut für Plasmaphysik, 85748 Garching, Germany
[2]Technische Universität München, 85748 Garching, Germany
[3]Forschungszentrum Jülich GmbH, Institut fuer Energie und Klimaforschung, Partner of the Trilateral Euregio Cluster (TEC), 52425 Juelich, Germany
[4]Lehrstuhl für Textilmaschinenbau und Institut für Textiltechnik (ITA), 52062 Aachen, Germany
[5]Institut für Textil- und Verfahrenstechnik, 73770 Denkendorf, Germany
[*]Present address: TEC-KNIT CreativCenter für technische Textilien GmbH, Am Böwing 10, 46414 Rhede

Corresponding author:
Hanns Gietl, Max-Planck-Institut für Plasmaphysik, 85748 Garching, Germany
Email: hanns.gietl@ipp.mpg.de

temperature range of CuCrZr alloy in a fusion reactor environment is 180 °C to 300 °C due to embrittlement under fusion neutron irradiation at lower and loss of strength at elevated temperature (5). Moreover, the combination of W and Cu alloys within a PFC bears engineering difficulties. On the one hand, it leads to significant thermal stresses during heat loading of the component as W and Cu have a high thermal expansion mismatch. On the other hand, the optimum operating temperature ranges of these materials do not overlap (cf. Fig. 1).

To overcome the limitations of monolithic W as PFM and Cu alloys as heat sink material, development efforts have been directed towards a W fibre-reinforced W (W_f/W) and W fibre-reinforced copper (W_f/Cu) metal matrix composite (MMC) (18; 19; 20). Within these composite materials, high strength - even at elevated temperature (21) - commercially available drawn W wire (OSRAM GmbH) is used as reinforcement. It has been demonstrated that W_f/W shows pseudo-ductile behaviour already at room temperature (22) which is based on extrinsic mechanisms (23; 19) similar to those exploited within ceramic fibre-reinforced ceramics (24). Besides short fibre reinforced W_f/W produced with a powder metallurgical process (25), a promising production route for W_f/W reinforced with continuous fibres is a layered chemical vapour deposition process (26; 18; 27; 19). A possible way of enhancing the high temperature strength of Cu based materials is the incorporation of W fibres into a Cu or Cu alloy matrix and to produce a W fibre-reinforced Cu (W_f/Cu) composite material. There is no mutual solubility between W and Cu but the wetting of liquid Cu on W is good which leads to a strong cohesion of the W fibres in the matrix. This results in a good stress transfer from the matrix to the fibres (28). Hence, W_f/Cu MMCs can be manufactured by means of liquid Cu melt infiltration of open porous W_f preforms (20). Furthermore, W_f/Cu offers some flexibility as properties, like the CTE, can be tailored through suitable arrangement of the reinforcing fibres.

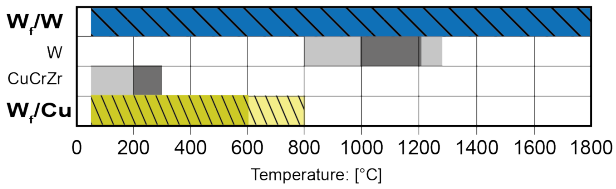

Figure 1. Optimal operating temperature ranges of the described metal matrix composites based on (18). The darker shaded areas represent the optimal operation temperature, while the lighter shaded areas correspond to the maximum operating temperate range. The temperature range of monolithic W and CuCrZr can be extended by the incorporation of W fibres as reinforcement. The data for W is based on (29) while the data of CuCrZr is based on (30).

The MMCs briefly described above are capable of minimizing the operating temperature gap between monolithic W and Cu and reducing the corresponding thermal expansion mismatch. In Fig. 2, possible PFC design concepts based on a W_f/W flat tile and mono-block design in combination with a W_f/Cu composite are shown. The PFM is in this case W_f/W which is joined (e. g. with a Cu based braze) to an actively cooled heat sink.

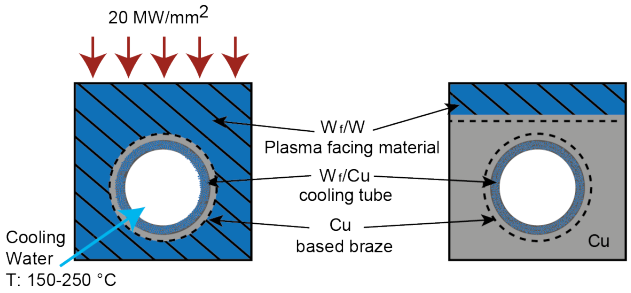

Figure 2. Conceptual mock-up designs based on mono-block (left) and flat tile (right) concepts utilizing W_f/W and W_f/Cu based on (18; 31).

As both materials are produced with different methods the challenges for the fibrous preform production differ significantly. For the favoured design concepts of W_f/W which is produced in plate form, flat fabrics with a unidirectional fibre arrangement and a narrow and defined fibre spacing are needed. As W_f/Cu is foreseen as heat sink material a pipe shaped fibrous preform is needed. Such W fibre preforms with these desired shapes are not commercially available. For that reason, well-established textile technological methods like weaving and braiding were adapted for W fibres and these are presented in this contribution. Moreover, it is important for the up-scaling of the material production to have reliable preform manufacturing processes. For further development, W fibre yarn was produced to improve the textile processability of the W fibre and to possibly strengthen the composites.

Tungsten fibres as reinforcement

W fibres are produced by wire drawing (32) and are commercially available down to a nominal diameter of 16 μm (OSRAM GmbH). W fibres show a high tensile strength (33), high stiffness and in contrast to conventional bulk W ductility even at room temperature (34). Due to the high degree of deformation during the drawing process W fibres exhibit an elongated grain structure (35; 32) which is shown in Fig. 3 and was identified as the key parameter for ductility and high strength (36).

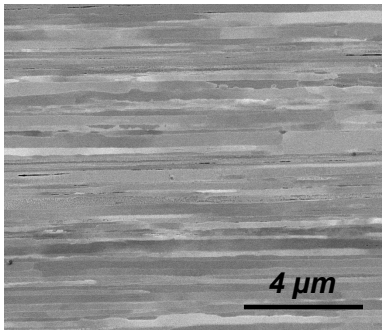

Figure 3. The fine elongated grain structure of an as-fabricated K-doped W fibre with a nominal diameter of 150 μm from a longitudinal backscattered SEM micro-section (37).

The strength of drawn W fibres increases with decreasing diameter (Tab. 1).

Table 1. Ultimate tensile strength dependence of drawn W fibres.

Diameter [μm]	Strength [MPa]
600	1765 (13)
150	2926 (36)
50	2935 (33)
20	3920 (13)
16	4500 (33)

The tensile behaviour of different diameter is qualitatively the same and the higher strength can be explained with the higher degree of deformation which leads to finer grains which have a beneficial influence on the ultimate tensile strength (33). Such fibres were originally produced for the lighting industry where the thermal and microstructural stability is essential (13; 38). For that reason, the fibres were doped with potassium and so called non-sag W was produced (39). The potassium forms bubbles at the grain boundaries while the W is heated. This leads to the pinning of the grains and a massive grain growth is suppressed. As massive grains within W fibres lead to embrittlement the temperature at which this growth starts is of great importance. Pure W fibres and potassium doped W fibres are ductile at room temperature (35). Pure W fibres are stable against embrittlement up to 1800 °C (36) whereas doped fibres embrittle only above 2200 °C (40), respectively. By using potassium as dopant, a slightly decreased ultimate tensile strength compared to pure W fibres was observed (40). In this contribution K-doped W fibres are used and exemplary stress-strain curves of these fibres are shown in Fig. 14.

Textile techniques

Planar fabrics for W_f/W plates

For W_f/W the preform must consist of unidirectionally arranged fibres with a defined fibre spacing in one plane. Flatness and spacing are necessary as the fibre arrangement has direct influence on the composite density. Inaccuracies such as unevenness and a too small fibre distance in the fibre arrangement can lead to premature blocking of the gas path as in the standard chemical vapor deposition (CVD) process W growths on all surfaces with the same rate. This gas path blocking leads to unfilled cavities which are visible as pores in W_f/W. In Fig. 7, the pore formation especially in fabric 1, 2 and 3 between the layers can be seen where the distances within a layer are smaller than in between the layers. The unidirectionality (UD) of the fibres is desired for the W_f/W production where W should be unidirectionally reinforced with W fibres. This allows an easier understanding of the acting mechanisms in this early development stage during mechanical testing (19). Moreover, such a fibrous preform is essential for the development of an automated continuous production process for W_f/W.
A specifically woven fabric can fulfil all the above mentioned requirements. In a fabric, two or more thread systems, the warp and weft threads being perpendicular to each other, form the woven fabric (see Fig. 6). Within such a fabric the weft and warp fibre distance can be adjusted. These threats can contain materials used for the textile production e.g. cotton fibres or materials for technical fabrics e.g. carbon fibres (41) or ceramic fibres (42). It is also possible to produce woven fabrics out of metal wires (43). In a shuttle loom weaving machine, the warp threads are running in the machine direction and through the reed which defines the distances between the treads and therefore the fabric density (44). With this method fabrics with a defined fibre distance where the fibres have a preferably direction can be produced and for the investigated W fabrics the weft wire distance is maximised as a UD fabric is needed.
For the fabrics presented in this paper a Mageba shuttle loom (type SL 1/80) weaving machine with 150 μm doped W fibres as warp fibre and a 50 μm doped W fibre as weft fibre were used. Moreover, the fabric density was modified with five different reeds (DERIX 400/10/240, DERIX 333/10/200, DERIX 285/10/170, DERIX 250/10/150 and DERIX 222/10/133) to identify the optimal warp fibre distance. The specifications are shown in table 2. With this set up 60 mm wide fabrics with a different amount of fibres were produced. The weave was performed of a creel and a plain pattern was chosen for the fabrics.

Table 2. Specifications for the different reeds used for the fabric manufacturing. All reeds had a width of 60 mm.

Reed Nr.	Fibres	Spacing of reed measured [mm]
1	240	0.10
2	200	0.13
3	170	0.18
4	150	0.22
5	133	0.27

As W fibres have a high stiffness the weft fibre does not enwind the warp fibre and the fabrics did not have the needed flatness. This problem is schematically shown in Fig. 4. It was solved by equipping the weaving machine with a roller to compress the fabrics and bend the weft fibres around the warp fibres.

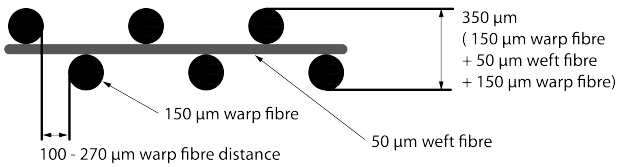

Figure 4. Schematic sketch of the fabrics without compression. The weft fibre is straight and does not bend around the warp fibres. Therefore, the fabric height is the sum of two times the warp fibre diameter and the weft fibre diameter.

A schematic sketch of the fabrics after the compression can be seen in Fig. 5. For each type, a constant thickness off around 200 μm was measured.

The five different fabrics are shown in Fig. 6. By comparing the spacings from the reeds (Tab. 2) and the measured fibre spacings (Tab. 3) it can be seen that the fibre spacings of the fabrics is always lower then the fibre spacing

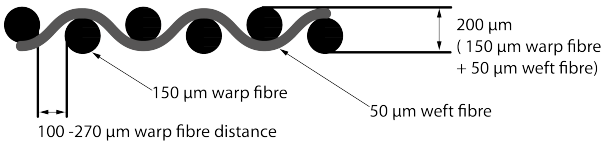

Figure 5. Schematic sketch of the fabrics after compression. The weft fibre is deformed and bend around the warp fibres. This results in a fabric hight of around 200 μm.

defined by the reed. This smaller fibre spacing is caused by the weft fibres pulling the warp fibres together. Moreover, by compressing the fabrics with the roller the weft fibre is deformed and shortened so the warp fibre spacing is getting even smaller. At the edge area of the fabrics this effect is more prominent.

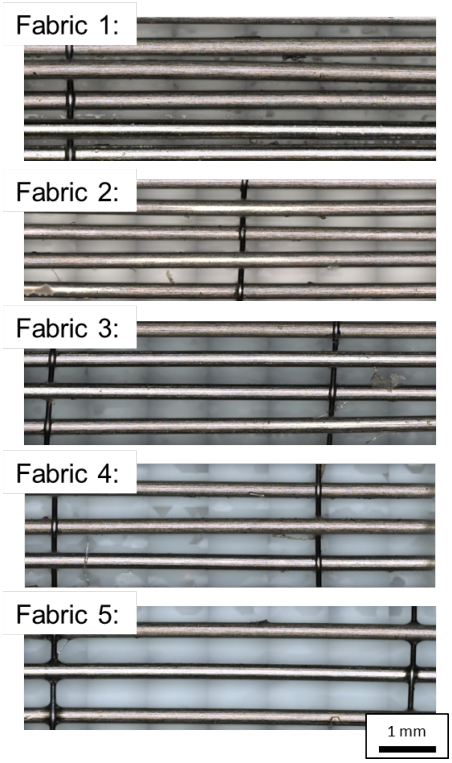

Figure 6. Optical images of W fabrics produced with different fibre spacings. The fibre spacing is increasing from fabric 1 to 5 and the values are shown in Tab. 3.

With the different fabrics illustrated in Fig. 6, a layerwise CVD process as described in (18; 19) was performed to produce a three layered W_f/W composite. This gives the opportunity to investigate the influence of the fabric type on the synthesis of W_f/W composite (Fig. 7) and thus to determine the optimal warp fibre distance. The weft fibre distance was adjusted to the maximal possible distances of around 30 mm. The density was measured using a cross-section image. This method uses a processed microscopy image to distinguish between the pores (converted to black) and the dense material (converted to white) by calculating the black and white pixels within that image. It was performed for one cross-section on each sample with a area of approximately 85 mm^2.

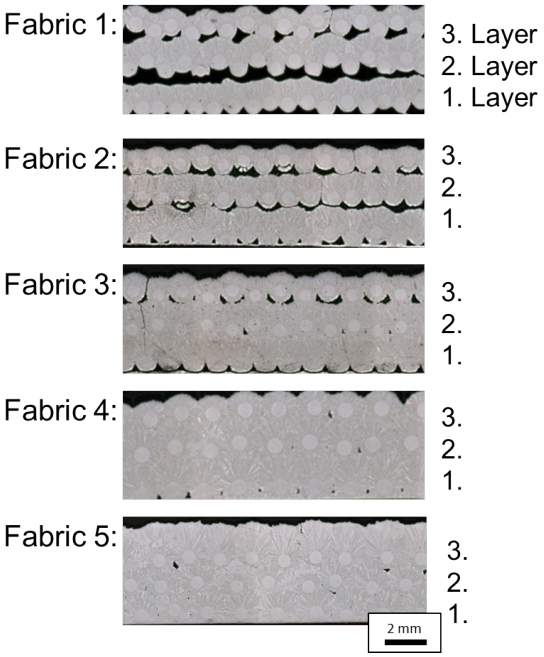

Figure 7. Optical images of three layer W_f/W produced with the different fabrics. The density of the composite is increasing with increasing fibre spacing. This results in a lower achievable fibre volume fraction. The values are shown in Tab. 3

For fabric 1, a low density with large pores between the layers and therefore a poor layer connectivity can be seen. A higher material density was achieved for fabric 2 and the pores are located between the layers. The W_f/W of fabric 3 shows small pores along the fibres with a lower amount of pores between the layers. The composites of fabric 4 and 5 have the lowest amount of pores but some small pores between the layers are still remaining. A comparison of fibre spacing and density is given in Tab. 3. Here, with a larger fibre spacing of the fabrics the density of the composite increases. However, a larger fibre spacing leads to a lower fibre volume fraction.

Table 3. The different fabrics with the corresponding warp fibre spacing (Fig. 6) and the density of the three layer W_f/W (Fig. 7). The values for the density were measured at one area of approximately 85 mm^2 for each sample. The achievable fibre volume fractions are calculated theoretical values.

Fabric	Wire Spacing measured	Density measured	achievable fibre volume fraction
1	90 $\pm$12 μm	83.8 %	30.6 %
2	113 $\pm$8 μm	92.9 %	25.5 %
3	158 $\pm$17 μm	96.5 %	18.6 %
4	204 $\pm$19 μm	99.3 %	14.4 %
5	271 $\pm$10 μm	99.7 %	10.1 %

As it was seen in previous studies (45; 46; 19), the CVD W grows with a constant rate on isothermal surfaces. Assuming that the fabric has a uniform temperature during deposition the CVD W will grow with the same rate on the fabric surfaces which are accessible to the process gases. For that reason the fibre spacing within a layer must be at least as large as the fibre diameter in order to archive a dense matrix. This implies that with a 150 μm fibre and a unidirectional fibre arrangement the smallest possible fibre distance is 150

μm. With these fibre distances a theoretical fibre volume fraction of 20 % is achievable. But as the fibre arrangement has always some inaccuracies, a nearly dens matrix was achieved with a fibre distance of around 200 μm. This leads to a theoretical maximum fibre volume fraction of over 14 % for the presented fabrics.

Circular W_f braidings for W_f/Cu tubes

The preforms for W_f/Cu need to exhibit a circular tube-like shape as this composite material is foreseen to form a cooling channel for an actively cooled component. In order to achieve such preforms circular braiding has been investigated.
Braiding in general is a well-established textile technique (47) in which yarn carriers rotate along a circular sinusoidal track while half the carriers rotate in a clockwise direction . The remaining half of the carriers rotates in a counterclockwise direction. As a result, the applied yarns interlace with each other at a biased angle to the braiding machine axis. The basic geometrical features which are the braid angle and the characteristic unit cell are schematically illustrated in Fig. 8 (47). If the circumference shall be reinforced a lower braiding angle is preferred. A higher braiding angle is desired if the axial direction of the composite needs reinforcement.

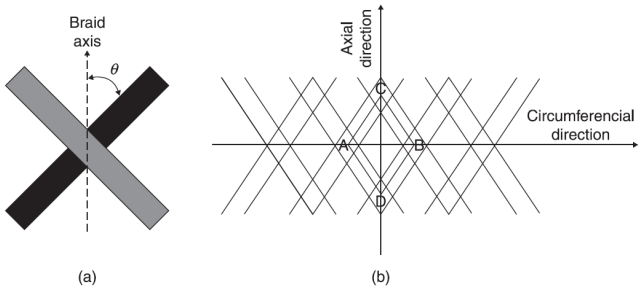

Figure 8. Schematic illustration of the geometry of a braided structure defining (a) the braid angle and (b) the characteristic unit cell (47).

The braiding machine that has been used for producing the preforms described within this work is a 48” vertical maypole braider (Körting Nachfolger Wilhelm Steeger GmbH & Co. KG). With this braider, multi-layered cylindrical W fibre preforms have been produced by means of mandrel overbraiding. The diameter of the used W fibres ranged from 150 μm down to 50 μm. In Fig. 9, images of two such circular braidings are shown.

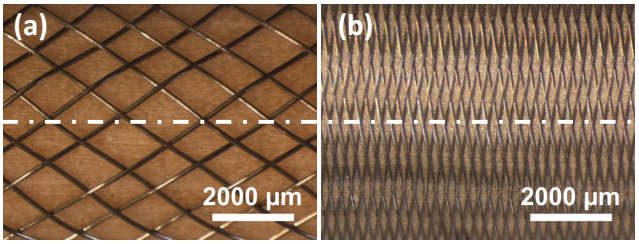

Figure 9. Microscopic images of regular biaxial circular braidings made out of drawn K-doped W fibres with a diameter of (a) 150 μm and (b) 50 μm.

Fig. 9(a) illustrates a braiding that consists of W fibres with a diameter of 150 μm while Fig. 9(b) shows a braiding that consists of W fibres with a diameter of 50 μm. It can be seen that the fibres with the smaller diameter of 50 μm are much more suited for such a processing as the braiding shows significantly less perturbing undulations which allows higher braiding angles and hence a higher braid cover factor to be achieved. This in turn means that the braid can provide better reinforcement in the circumferential direction.
Following these results, multi-layered circular braidings as preforms for composite material fabrication have been manufactured successfully. In Fig. 10, two such preforms with different architecture are illustrated. They are both manufactured from the same W fibres with a diameter of 50 μm. Fig. 10(a) shows a multilayered preform with a braiding angle of approximately 60° while Fig. 10(b) illustrates a braiding with a significantly lower braiding angle of about 12° defined according to Fig. 8(a). These preforms demonstrate the direct possibility to influence the preform architecture and hence the later composite material properties by varying the braiding parameters during the preform production process.

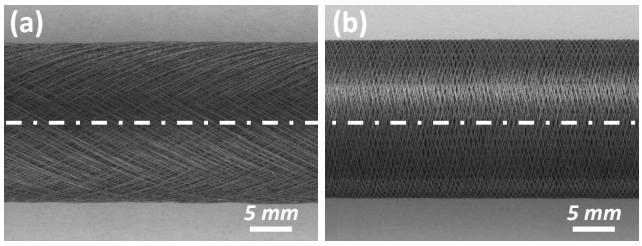

Figure 10. Images of multi-layered circular braidings as preforms for W_f/Cu fabrication made of drawn K-doped W fibres with a diameter of 50 μm with a braiding angle of (a) ca. 60° and (b) ca. 12° (according to Fig. 8(a)).

It has been demonstrated that preforms as illustrated in Fig. 10 can be used to produce W_f/Cu by means of liquid Cu melt infiltration as exemplarily shown in Fig. 11 (20). With such a Cu melt infiltration process it is possible to produce a pore free Cu matrix around the multi-layered circular braidings which is needed in order to achieve good thermomechanical properties of the composite.

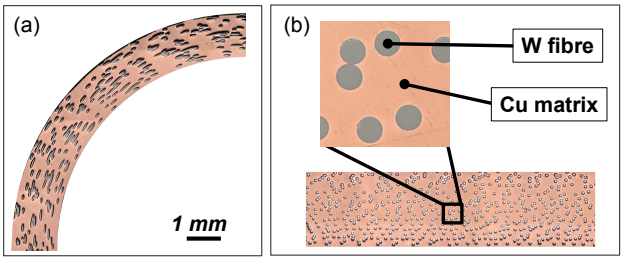

Figure 11. Exemplary microsections of a W_f/Cu pipe ((a) transversal, (b) axial) manufactured by means of liquid Cu melt infiltration of a braided preform as illustrated in Fig. 10 (b) (20).

Yarn fabrication

W fibres with a smaller diameter have a higher strength and can therefore lead to improved performance compared to the up to now produced W_f/W and W_f/Cu. The handling

of such thin fibres during the manufacturing with standard textile machine leads to problems. Thin single fibre can only withstand low loads - below 1 N for 16 μm (33)- and could fail during processing. The use of a yarn construction from multiple thin fibres would overcome this problem and lead to the following potential advantages. On the one hand, overall strength is increasing with decreasing diameter which could lead to an increased overall strength of the compound. On the other hand, a yarn from multiple filaments shows a much lower bending rigidity than a single fibre which would consequently increase the handling in textile processes.
To create a stable yarn compound the filaments can either be twisted or covered/enwinded by another material. W fibres have high moment of inertia compared to polymer fibres as the mass density of tungsten ($\sim$19,250 g/cm^3 (13)) is much higher compared to any polymer ($<$2 g/cm^3 (48)) used as reinforcement. Therefore, a yarn created in a one-step twisting process tends to curl in untensioned condition. The processability of such a yarn in textile production processes is not given as they tend to move uncontrolled in the later textile product. Moreover, the W fibres have to remain straight during the process as the flatness is crucial for the fabrics. For a covering of the filaments with staple fibres the surface of W is too smooth. Therefore, in this work an enwinding process is used. W filaments are enwinded by a polymer yarn. This yarn needs to be removable after textile processing as it does not withstand the high manufacturing temperatures of the composites. A schematical illustration of a W yarn enwinded with a polyvinyl acetate (PVA) multifilament is shown in Fig. 12.

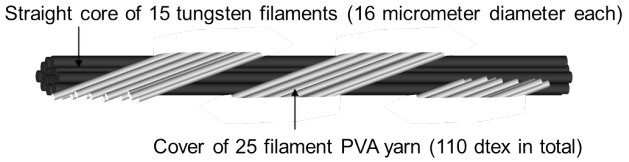

Figure 12. Schematical illustration of a W yarn enwinded with a PVA multifilament consisting of 15 W filaments with a diameter of 16 μm.

For the yarn production an enwinding machine Allma ESP2 from Saurer AG, Watwill, Switzerland was used. These machine allows to guide a staple fibre roving through a drafting unit and enwind it afterwards using a staple fibre or fibre yarn. In this work 15 W filaments with a diameter of 16 μm each were fed into the machine in parallel. The drafting unit was bypassed since no draft of the yarn thread is needed. Afterwards the fibres were enwinded by a PVA multifilament (Solvron SF 110T/25F, NITIVY CO.,LTD, Tokyo)and the applied number of twists per meter was 250 Tw/m. The resulting enwinded W yarn with and without the PVA multifilament are shown in Fig. 13. The as-fabricated yarn with the PVA multifilament has a diameter of arround 150 μm while pure yarn without the multifilament has a diameter of arround 70 μm.

Tensile tests were performed on the produced yarn. A force of 14.07 $\pm$ 0.13 N (mean value of 13 tensile tests with standard deviation) is needed to break the yarn within the tensile test where the displacement was recorded with a contact-free optical measurement method. The calculated

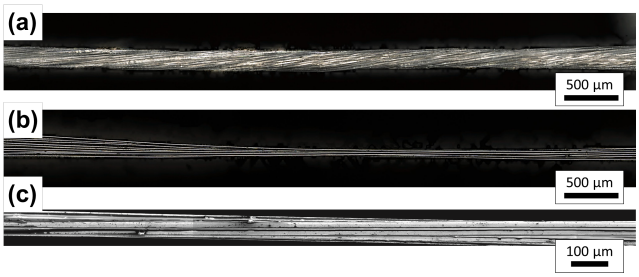

Figure 13. W yarn: 15 W filaments (16 μm diameter); (a) enwinded with a PVA multifilament and a diameter of arround 150 μm (confocal laser scanning microscope image) (b) and (c) without PVA multifilament and a diameter of arround 70 μm (b) CLSM image, (c) SEM image).

overall strength is 4666 $\pm$ 42 MPa at which the area was calculated by summing up the area of the 15 W filaments. In Fig. 14 a representative stress-strain curve is shown. The linear loading of the yarn is followed by a non-linear region which leads to a plateau-like region of the curve. This is followed by the maximum load of the yarn which then fails stepwise. This indicates that the single filaments in the yarn do not fail at once. There might be friction within the yarn caused by the manufacturing process which leads to a twist of the yarn which can be seen in Fig. 13 (b) and (c). The fracture strain of the yarn is 2.1 $\pm$ 0.3 % and the stress-strain curve is qualitatively comparable with the known W fibres (36; 33), except of the stepwise failure. Moreover, it can be seen that the strength is slightly higher compared with results of 16 μm single filament of W from literature (33) and over 1000 MPa higher than the results obtained for 150 μm W fibres (36).

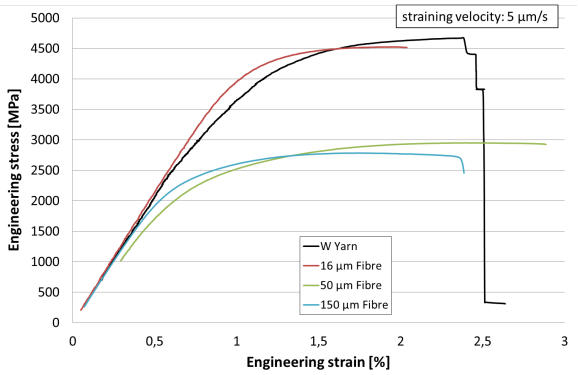

Figure 14. Representative stress-strain curve of a yarn (black) with stepwise failure after the ultimate tensile strength is reached. Exemplary stress-strain curves of K-doped W single fibres with 16 (red), 50 (green) and 150 (blue) μm diameter.

In Fig. 15, the fracture surface of such a W yarn can be seen in an SEM image. In this yarn all single filaments failed in one plane which was only the case for a few yarns while the filaments of the most yarns failed on variable positions over the hole gauge length. This example was chosen as the typical reduction in diameter as well as the knife edge fracture surface (35) for the 15 W filaments is visible. The fracture surfaces of the single filaments and the stress-strain behaviour indicates that the W fibres within the yarn act like single fibres under tension load and do not show any degradation during the yarn production. However,

the manufacturing routines for the composites might change because of the arrangement of the single filaments. This might not be an issue for W_f/Cu as melted Cu infiltrates even tiny cavities. In contrast to that, the chemical vapor deposition process for W_f/W might be changed to an chemical vapor infiltration process as the process gas needs to access every cavity.

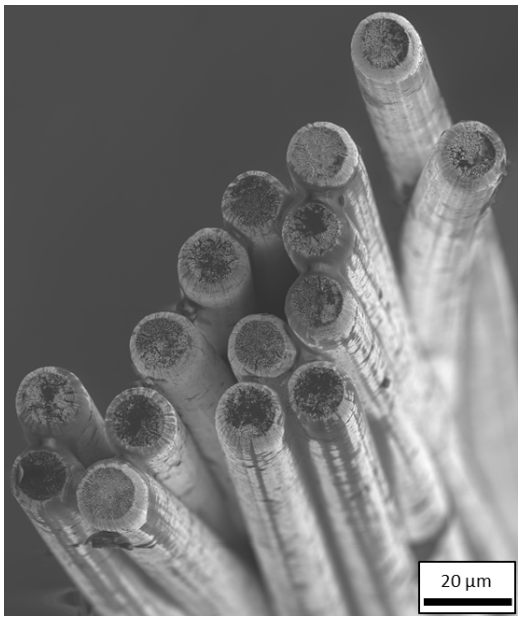

Figure 15. Fracture surface of one yarn where all single filaments failed in one plane with the typical necking and knife edge fracture surface obtained from an SEM image.

Summary and Outlook

In this contribution we showed the W fibre preform production for the use in W_f/W and W_f/Cu MMC which are produced with a layerd CVD and Cu melt infiltration process, respectively. These textile products are essential for the MMC production. As the W fibres have a high stiffness, the processability with standard textile techniques is comparable with carbon or ceramic fibres. The high stiffness was the biggest issues during the weaving and braiding of the fibres and can be mitigated by choosing fibres with a smaller diameter. The high ductility and damage tolerance of W fibres on the other hand was beneficial for the use in standard weaving and braiding machines. For the first time, W fibre fabrics were specifically produced for the use in W_f/W composite production. It was shown that with the variation of the fibre architecture, especially the fibre distance, a pore free and dense composite can be produced. This allows to fabricate W_f/W in a more standardized and faster way. Moreover, the implementation of a pressing step after the weaving process leads to a flat fabric. It has been found that for the first fabric production the warp fibre with 150 μm, the weft fibre with 50 μm and a fibre distance of around 200 μm leads to the best possible W_f/W composite material with a relatively low fibre volume fraction but with a nearly dense matrix material.
Furthermore, it has successfully been demonstrated that drawn W fibres can be processed textile technologically to multilayered preforms for W_f/Cu fabrication by means of circular braiding which is a well-established and industrially viable technique. In this regard, it has been found that W fibres with diameters $\leq$ 100 μm are suited for such a processing technology as they exhibit sufficient flexibility in order to achieve braidings with small undulations as well as low braiding angles. With such multilayered braided preforms pore free W_f/Cu has successfully been produced.
The production of a stable yarn from W filaments with a diameter of 16 μm is possible by enwinding with a PVA. The W fibre remains straight while the PVA multifilament is removable after textile fabric production. The yarn has a higher overall strength than a single fibre of a comparable diameter and can therefore take higher loads in W_f composites.

- fabric as suitable preform for W_f/W developed (over 99% dense composite)
- multilayered braiding as suitable preform for W_f/Cu developed (pore free composite)
- W yarn production routine established (increased load bearing for future W_f/W and W_f/Cu)

For the further development this yarn will be implemented in the W fabric and braiding production. Furthermore, it is necessary to design a continuous layer deposition process for the production of W_f/W and to show the possibility of a large scale production. Finally, the combination of the two described MMCs could help to overcome the operation temperature gap of monolithic W and Cu in order to produce a damage resilient PFC for future fusion devices.

Acknowledgement

The authors want to acknowledge the Osram GmbH, Schwabmünchen, Germany for providing the W wire and the whole W_f/W team for fruitful discussions. This work has been carried out within the framework of the EUROfusion Consortium and has received funding from the Euratom research and training programme 2014-2018 under grant agreement No 633053. The views and opinions expressed herein do not necessarily reflect those of the European Commission. Furthermore was this work supported by the JARA Energy Seed-Fund.

References

[1] McCracken GM and Stott PE. *Fusion: The energy of the universe*. 2. ed. Amsterdam, Netherlands: Academic Press, 2013. ISBN 0123846560.

[2] EFDA. *Fusion Electricity - A roadmap to the realisation of fusion energy*. 2012. ISBN 978-3-00-040720-8.

[3] Federici G, Bachmann C, Biel W et al. Overview of the design approach and prioritization of R&D activities towards an EU DEMO. *Fusion Engineering and Design* 2016; 109: 1464 – 1474. DOI:http://dx.doi.org/10.1016/j.fusengdes.2015.11.050. URL http://www.sciencedirect.com/science/article/pii/S0920379615303835.

[4] Team J et al. Fusion energy production from a deuterium-tritium plasma in the JET tokamak. *Nuclear Fusion* 1992; 32(2): 187.

[5] Stork D, Agostini P, Boutard J et al. Developing structural, high-heat flux and plasma facing materials for a near-term DEMO fusion power plant: The EU assessment. *Journal of Nuclear Materials* 2014; 455: 277 – 291.

[6] You J, Visca E, Bachmann C et al. European DEMO divertor target: Operational requirements and material-design interface. *Nuclear Materials and Energy* 2016; 9: 171 – 176. DOI:http://dx.doi.org/10.1016/j.nme.2016.02.005. URL http://www.sciencedirect.com/science/article/pii/S2352179115300788.

[7] Stork D, Agostini P, Boutard J et al. Materials R&D for a timely DEMO: Key findings and recommendationsof the EU roadmap materials assessment group. *Fusion Engineering and Design* 2014; 89: 1586 – 1594.

[8] You J, Mazzone G, Visca E et al. Conceptual design studies for the European DEMO divertor: Rationale and first results. *Fusion Engineering and Design* 2016; 109: 1598 – 1603. DOI:http://dx.doi.org/10.1016/j.fusengdes.2015.11.012. URL http://www.sciencedirect.com/science/article/pii/S0920379615303331.

[9] Gilbert M and Sublet JC. Neutron-induced transmutation effects in W and W-alloys in a fusion environment. *Nuclear Fusion* 2011; 51(4).

[10] Gilbert M, Dudarev S, Nguyen-Manh D et al. Neutron-induced dpa, transmutations, gas production, and helium embrittlement of fusion materials. *Journal of Nuclear Materials* 2013; : 755–760.

[11] Hirai T, Escourbiac F, Carpentier-Chouchana S et al. ITER tungsten divertor design development and qualification program. *Fusion Engineering and Design* 2013; (88): 1798–1801.

[12] Bolt H, Barabash V, Federici G et al. Plasma facing and high heat flux materials-needs for ITER and beyond. *Journal of Nuclear Materials* 2002; 307: 43–52.

[13] Lassner E and Schubert WD. *Tungsten - Properties, Chemistry, Technology of the Element, Alloys, and Chemical Compound*. Springer, 1999.

[14] Linsmeier C, Rieth M, Aktaa J et al. Development of advanced high heat flux and plasma-facing materials. *Nuclear Fusion* 2017; 57(9). URL http://stacks.iop.org/0029-5515/57/i=9/a=092007.

[15] J Boscary et al. Design improvement of the target elements of Wendelstein 7-X divertor. *Fusion Engineering and Design* 2012; 87(7–8): 1453–1456. DOI:10.1016/j.fusengdes.2012.03.034. URL http://www.sciencedirect.com/science/article/pii/S0920379612002372.

[16] M Matsukawa et al. Status of JT-60SA tokamak under the EU-JA Broader Approach Agreement. *Fusion Engineering and Design* 2008; 83(7-9): 795–803. DOI:10.1016/j.fusengdes.2008.06.047.

[17] M Missirlian et al. The WEST project: Current status of the ITER-like tungsten divertor. *Fusion Engineering and Design* 2014; 89(7–8): 1048–1053. DOI:10.1016/j.fusengdes.2014.01.050. URL http://www.sciencedirect.com/science/article/pii/S0920379614000519.

[18] Riesch J, Aumann M, Coenen J et al. Chemically deposited tungsten fibre-reinforced tungsten - the way to a mock-up for divertor applications. *Nuclear Materials and Energy* 2016; In Press.

[19] Gietl H, Riesch J, Coenen J et al. Tensile deformation behavior of tungsten fibre-reinforced tungsten composite specimens in as-fabricated state. *Fusion Engineering and Design* 2016; 124: 396–400.

[20] Müller A, Ewert D, Galatanu A et al. Melt infiltrated tungsten–copper composites as advanced heat sink materials for plasma facing components of future nuclear fusion devices. *Fusion Engineering and Design* 2017; 124: 455–459. DOI:10.1016/j.fusengdes.2017.01.042.

[21] Terentyev D, Riesch J, Lebediev S et al. Mechanical properties of as-fabricated and 2300 °C annealed tungsten wire tested up to 600 °C. *International Journal of Refractory Metals and Hard Materials* 2017; 66: 127–134.

[22] Gietl H, Olbrich S, Riesch J et al. Estimation of fracture toughness of tungsten fibre-reinforced tungsten composites. *In Preperation* 2018; In Preperation.

[23] Riesch J, Höschen T, Linsmeier C et al. Enhanced toughness and stable crack propagation in a novel tungsten fibre-reinforced tungsten composite produced by chemical vapour infiltration. *Physica Scripta* 2014; T159: 014031.

[24] Evans A. Perspective on the development of high-toughness ceramics. *Journal of American Ceramic Society* 1990; 73: 187–206.

[25] Mao Y, Coenen J, Riesch J et al. Development and characterization of powder metallurgically produced discontinuous tungsten fiber reinforced tungsten composites. *Physica Scripta* 2017; (T170): 014005.

[26] Neu R, Riesch J, Müller A et al. Tungsten fibre-reinforced composites for advanced plasma facing components. *Nuclear Materials and Energy* 2016; (12): 1308–1313.

[27] Riesch J, Coenen J, Gietl H et al. Tungsten fibre-reinforced tungsten composite - development of a new high performance material. *ECCM 2016 - Proceeding of the 17th European Conference on Composite Materials* 2016; .

[28] Herrmann A. *Interface Optimization of Tungsten Fiber-Reinforced Copper for Heat Sink Application*. PhD Thesis, Technische Universität München, 2009.

[29] Zinkle S and Ghoniem N. Operating temperature windows for fusion reactor structural materials. *Fusion Engineering and Design* 2000; 51-52: 55–71.

[30] Timmis W. Material assessment report on the use of copper alloys in DEMO. *Technical Report, Culham Centre for Fusion Energy* 2012; .

[31] Coenen J, Jasper B, Gietl H et al. Tungsten fibre-reinforced tungsten composites. *19th Plansee Seminar conference proceedings* 2017; .

[32] Schade P. 100 years of doped tungsten wire. *International Journal of Refractory Metals and Hard Materials* 2010; 28: 648660.

[33] Riesch J, Feichtmayer A, Fuhr M et al. Tensile behaviour of drawn tungsten wire used in tungsten fibre-reinforced tungsten composites. *Physica Scripta* 2017; (T170): 014032.

[34] Riesch J, Almannstötter J, Coenen J et al. Properties of drawn W wire used as high performance fibre in tungsten fibre-reinforced tungsten composite. *IOP Conference Series: Materials Science and Engineering* 2016; 136: 012043.

[35] Leber S, Tavernelli J and White D. Fracture modes in tungsten wire. *Journal of the Less Common Metals* 1976; 48: 119–133.

[36] Zhao P, Riesch J, Höschen T et al. Microstructure, mechanical behavior and fracture of pure tungsten wires after different heat treatments. *International Journal of Refractory Metals and Hard Materials* 2017; 68: 29–40.

[37] Müller M, Ilg M, Gietl H et al. The effects of heat treatment at temperatures of 1100 °C to 1300 °C on the tensile properties of high-strength drawn tungsten fibres. *Nuclear Materials and Energy* 2018; (submitted).

[38] Yih W and Wang C. *Tungsten: Sources, Metallurgy, Properties, and Applications*. Springer US, 1979.

[39] Pink E and Bertha L. *Metallurgy of Doped/Non-Sag Tungsten*, volume 1. Springer Netherlands, 1989.

[40] Riesch J, Han Y, Almannstötter J et al. Development of tungsten fibre-reinforced tungsten composites towards their use in DEMO - potassium doped tungsten wire. *Physica Scripta* 2016; T167: 014006.

[41] *CARBON AND HIGH PERFORMANCE FIBRES. Vol. 6*. Chapman & HalI, 1995.

[42] Mouchon E and Colomban P. Oxide ceramic matrix/oxide fibre woven fabric composites exhibiting dissipative fracture behaviour. *Composites* 1995; 26: 175–182.

[43] Roh JS, Chi YS, Kang TJ et al. Electromagnetic shielding effectiveness of multifunctional metal composite fabrics. *Textile Research Journal* 2008; 78(8): 825–835.

[44] Greis T, Veit D and Wulfhorst B. *Textile Technology*. Hanser Fachbuchverlag, 2015.

[45] Riesch J. *Entwicklung und Charakterisierung eines wolframfaserverstärkten Wolfram-Verbundwerkstoffs*. PhD Thesis, Technische Universität München, 2012.

[46] Riesch J, Höschen T, Galatanu A et al. Tungsten-fibre reinforced tungsten composites: A novel concept for improving the toughness of tungsten. In *Proceedings of the Eighteenth International Conference on Composite Materials, Jeju, South Korea*.

[47] Potluri P and Nawaz S. Developments in braided fabrics. In *Specialist Yarn and Fabric Structures*. Elsevier. ISBN 9781845697570, 2011. pp. 333–353. DOI:10.1533/9780857093936.333.

[48] Chawla KK. *Fibrous Materials*. 2. ed. Cambridge University Press, 2016.